Glassy magnetic behavior induced by Cu^{2+} substitution in the frustrated antiferromagnet $ZnCr_2O_4$

J. Phys.: Condens. Matter **20** (2008) 255203 (8pp) doi:10.1088/0953-8984/20/25/255203

Glassy magnetic behavior induced by Cu^{2+} substitution in the frustrated antiferromagnet $ZnCr_2O_4$

Li-qin Yan[1], Ferran Maciá[2], Zhong-wei Jiang[1], Jun Shen[1], Lun-hua He[1] and Fang-wei Wang[1]

[1] State Key Laboratory of Magnetism, Beijing National Laboratory for Condensed Matter Physics, Institute of Physics, Chinese Academy of Sciences, Beijing 100080, People's Republic of China

[2] Departament de Fsica Fonamental, Facultat de Fsica, Universitat de Barcelona, Avenida Diagonal 647, Planta 4, Edifici nou, 08028 Barcelona, Spain

E-mail: lqyan@aphy.iphy.ac.cn

Received 12 February 2008, in final form 8 April 2008
Published 19 May 2008
Online at stacks.iop.org/JPhysCM/20/255203

Abstract

The structure and magnetic properties of the compounds $Zn_{1-x}Cu_xCr_2O_4$ (ZCCO) are investigated systematically. A structural phase transition from space-group symmetry $Fd3m$ to $I4_1/amd$ is observed in ZCCO. The critical value of the doping, x, appears at 0.58–0.62 through the appearance of a splitting of diffraction peaks at room temperature. Measurements of dc magnetization, ac susceptibility, memory effect and exchange-bias-like (EB-like) effect have been performed to reveal the glassy magnetic behaviors of ZCCO. The system with $x \leqslant 0.50$ suggests a spin glass-like (SG-like) magnetic characterization whereas doping values of $0.58 \leqslant x \leqslant 0.90$ define the system as 'cluster-glass-like' (CG-like) with unidirectional anisotropy. The Cu content suppresses the geometrical frustration of $ZnCr_2O_4$, which may correlate with the pinning effect of the Cu sublattice on the Cr sublattice to a preferential direction.

(Some figures in this article are in colour only in the electronic version)

1. Introduction

The 'magnetic geometrical frustration' where lattice geometry results in frustration of the antiferromagnetic (AFM) exchange interaction is one of the exciting topics of research in modern condensed matter physics [1]. It has been largely studied and observed in systems of spinels, pyrochlores and kagome lattices [2–4]. Among these systems, the AFM chromium spinel oxides AB_2O_4, composed by AO_4 tetrahedra and BO_6 octahedra, have attracted a considerable interest [5–8]. One example is the case of $ZnCr_2O_4$ [5–11], where Zn-site ions form a diamond lattice and a strongly geometrical frustration (frustration factor ≈31, defined by $f = |\Theta_{CW}/T_N|$) dominates spins residing on octahedral Cr sites with half-filled t_{2g} orbitals, forming a lattice equivalent to the pyrochlore structure. With cooling, this magnet undergoes a spin-Peierls-like phase transition ($T_N = 12.5$ K) with AFM order and a tetragonal structural distortion, together with a relief of the geometrical frustration.

The spin-glass (SG) property in geometrical frustrated magnets has also been extensively studied for many years [12–19]. It has shown that, experimentally and theoretically, the ground state degeneracy in geometrical frustration can be removed by atomic disorder or bond disorder leading to an SG type of ordering [17, 20–22]. It is known that the presence of the disorder, coming from either the site disorder or the competing interaction between AFM and ferromagnetism (FM), often generates a conventional SG (CSG) state. However, systems which possess disorder and highly geometric frustration often display some unconventional SG behavior, usually named 'geometrical SG (GSG)'. A recent study on magnetic ion Cu^{2+} substitution for Cd^{2+} ions in the $CdCr_2O_4$ series (CCCO) has revealed the structural phase transition from cube to tetrahedron at

$x = 0.64$ [24]. $Cd_{0.5}Cu_{0.5}Cr_2O_4$ shows a transition induced by magnetic field from a nonequilibrium SG state to a possible AFM/FM phase separation [23]. At the same time, magnetic ion substitution for non-magnetic ions is proposed as a feasible method to partially destroy the magnetic frustration through the pinning effect of the magnetic ions on the magnetic frustrated sublattice [2, 24, 25]. This pinning effect would establish a preferential orientation within the frustrated sublattice.

However, extensive studies on other compounds of this family are still lacking, and it is of interest to intensify studies in this direction; in particular, magnetic properties of signatures of tetrahedral structures (such as higher Cu substitution for Cd) have been rarely reported. In the present article, we have subjected $Zn_{1-x}Cu_xCr_2O_4$ (ZCCO) to detailed study of structure and magnetic properties by dc and ac magnetic measurements, isothermal magnetization (M), memory effect and exchange-bias-like effect. A structural phase transition and an evolvement of magnetic glassy behavior with Cu concentration are revealed.

The paper is organized as follows. In the next section (section 2), we detail the characteristics of the samples as well as the parameters and equipment used in all different measurements. In section 3 we show the structural phase transition and corresponding analysis via Rietveld refinement (A), the dc magnetic characterization (B), the studies of the ac susceptibility of the samples $Zn_{0.7}Cu_{0.3}Cr_2O_4$, $Zn_{0.5}Cu_{0.5}Cr_2O_4$ and $Zn_{0.1}Cu_{0.9}Cr_2O_4$ (C), the memory effect in the sample of $Zn_{0.5}Cu_{0.5}Cr_2O_4$ (D) and the EB-like effect of $Zn_{0.1}Cu_{0.9}Cr_2O_4$ (E). In section 4 we discuss the results exposed and, finally, we summarize and conclude our study in section 5.

2. Experiment

2.1. Sample preparation

The polycrystalline samples of ZCCO with $x = 0$, 0.1, 0.3, 0.5, 0.58, 0.60, 0.62, 0.64, 0.66, 0.68, 0.70, and 0.90 have been prepared by using standard solid-state reactions of ZnO (99.99%), CuO (99.995%), and Cr_2O_3 (99.98%) powders from Alfa Aesar as starting materials. Once the stoichiometric powder mixtures were well ground, the mixture was heated according to the following schedule in air: 4 °C min^{-1} up to 200 °C, holding 30 min, and 4 °C min^{-1} up to 830 °C, holding 240 min. The resultant mixtures were reground, pelletized, and then sintered for 4320 min at 950 °C with subsequent slow cooling to room temperature. Then the compounds were reground and reheated at 980 °C for 7200 min. A black product with a spinel structure was obtained. The powder x-ray diffraction (XRD) pattern confirmed that the final product has a cubic-type spinel single phase for $0 \leqslant x \leqslant 0.5$ and tetragonal-type spinel single phase for $0.58 \leqslant x \leqslant 0.9$.

2.2. Structural analysis

X-ray powder diffraction experiments were performed by using a Rigaku diffractometer equipped with a monochromator (Cu Kα radiation, 40 kV, 120 mA). Diffraction data were collected at room temperature in the angle (2θ) range from 10° to 80° with a step of 0.02°. The counting time was 2 s for each step. Crystallographic parameters were analyzed by Rietveld full-profile refinement using the Fullprof program [26].

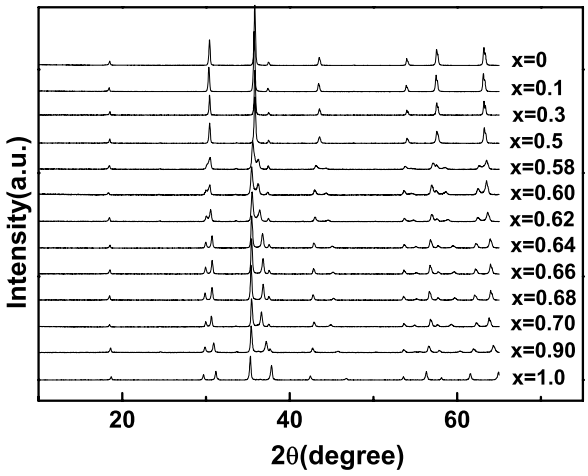

Figure 1. XRD patterns for all ZCCO compounds.

2.3. Magnetic measurements

The temperature and field dependences of the magnetization were measured by using a commercial superconducting quantum interference device magnetometer (MPMS-7, Quantum Design). For the dc magnetization temperature curves, measurements were performed after zero field cooling (ZFC) and field cooling (FC) in a fixed field (500 Oe). The magnetization curves for all samples were measured at 5 K and in the magnetic field range from 0 to 5 T, 5 to −5 T, then −5 to 5 T to detect the coercive field. For clarity, we show the curves only from 0 to 5 T in the paper. Ac susceptibility measurements were made using a Physical Property Measurement System (Quantum Design). The data were collected after ZFC. Memory effect and EB-like effect measurements were also performed by MPMS-7, Quantum Design.

3. Results

3.1. Crystal structures

For clarity, figure 1 shows the powder XRD patterns only within the range from $2\theta = 10°$ to 65° for all the studied ZCCO compounds. It is clear that the diffraction single peaks of 30°, 36°, 43°, 54°, 58° and 63° split into double peaks with increasing copper dopant, which indicates that a structural phase transition has occurred. To determine accurate lattice parameters and atomic positions, Rietveld analysis was carried out for all the powder XRD data. The structural phase with space group $Fd3m$ and the initial sets of Zn(Cu) at 8a (1/8, 1/8, 1/8), Cr at 16d (1/2, 1/2, 1/2) and O at 32e(x, x, x) changes into a new phase with space group $I4_1/amd$ and sets of Zn(Cu) at 4a (0, 1/4, 7/8), Cr at 8d (0, 1/2, 1/2) and O at 16e (0, y, z) within the range $0.58 \leqslant x \leqslant 0.62$. Notice that previous study in the $Cd_{1-x}Cu_xCr_2O_4$ (CCCO) series [23] showed that CCCO

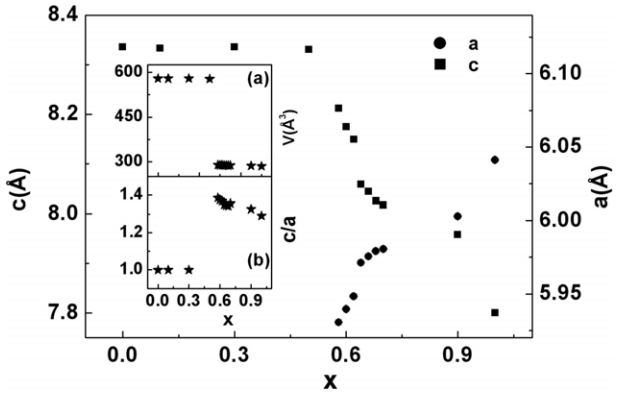

Figure 2. x dependence of crystal lattice parameters. The insets display the x dependence of (a) volume and (b) c/a.

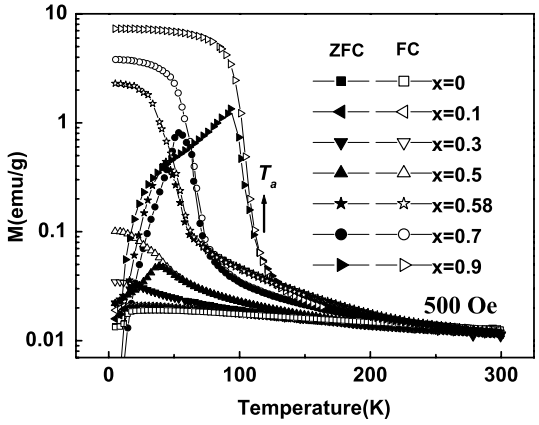

Figure 3. Temperature dependence of ZFC and FC magnetization for ZCCO compounds under the magnetic field of 500 Oe.

underwent a phase transformation from cubic ($Fd3m$) to tetragonal ($I\bar{4}2d$) at a Cu concentration of $x = 0.64$. This distortion was associated with the big difference in the ionic radii (Cd^{2+}: 0.97 Å, Cu^{2+}: 0.72 Å) and the Jahn–Teller effect of Cu^{2+} ions [27]. Compared with the noncentrosymmetric ($I\bar{4}2d$) transition of the CCCO series [23], the phase transition to $I4_1/amd$ in ZCCO is more centrosymmetric (two less alterable coordination parameters: X_{Cr} and X_O), attributable to the smaller difference of ionic radii on A sites of Zn^{2+} (0.74 Å) compounds compared with Cd^{2+} (0.97 Å) ones. The results of the lattice parameters and unit cell volume are plotted in figure 2 as a function of the Cu concentration. An abrupt drop in cell volume (see inset (a) of figure 2) is observed at $x = 0.58$, which is a result of the smaller size of the ionic radius of Cu^{2+} (0.72 Å) compared with Zn^{2+} (0.74 Å). This contraction corresponds to the compression of the c axis and a slight expansion of the a and b axes (see figure 2), indicating that the ZCCO structure is distorted from cube to tetrahedron at $x = 0.58$. The distorted feature, c/a, first increases abruptly, then decreases with the increasing Cu content (see inset (b) of figure 2), suggesting that the most distorted case occurs at $x = 0.58$ with $c/a = 1.385$.

3.2. Magnetization

Figure 3 presents the dc magnetic measurements for different Cu contents $x = 0$, 0.1, 0.3, 0.5, 0.58, 0.7, and 0.9 of the $M_{ZFC}(T)$ and $M_{FC}(T)$ under an applied field of 500 Oe. When the sample is doped with $0.58 \leqslant x \leqslant 0.9$, going from high to low temperatures, the $M_{ZFC}(T)$ increases till a maximum and then drops down with a small or an obvious change in the downward trend below ~50 K until the lowest temperature, $T = 5$ K. The $M_{ZFC}(T)$ and $M_{FC}(T)$ have the same values for temperatures above T_a (defined as the bifurcation temperature between ZFC and FC curves). Below this temperature, $M_{FC}(T)$ rises more rapidly until a certain point, from where it still has a slowly upward trend until 5 K. T_a shifts to higher temperatures with higher x. Such a large bifurcation between ZFC and FC curves is a hint at the existence of a short-range-ordered cluster, as observed in some perovskites [28–30]. When the samples are doped with $0 \leqslant x \leqslant 0.5$, with decreasing Cu content, the difference between

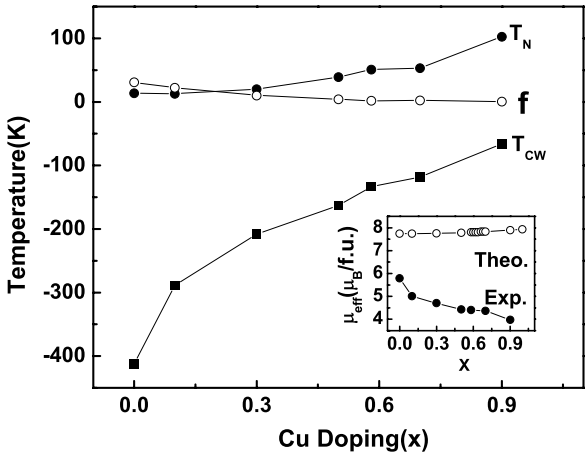

Figure 4. x dependence of Curie temperature T_N, Curie–Weiss temperature T_{CW} and frustration factor f. The inset shows the x dependence of effective magnetic moment per formula theoretically and experimentally.

cusp temperature and T_a in $M_{ZFC}(T)$ curves is reduced and even coincides at $x = 0$, indicating now the reduction of the number of short-range-ordered clusters and the emergence of SG-like behavior.

The magnetization data above 200 K can be well fitted, for all samples, using the Curie–Weiss law with the expression $\chi^{-1} = (T - \theta)/C$, where θ denotes the Weiss constant and C is the Curie constant. Figure 4 shows the corresponding fitting parameters. One can see that both the Curie–Weiss temperature and the Néel temperature (defined as the maximum value of $|dM/dT|$) increase with x, suggesting an increase of the ferromagnetic interaction contributed from the Cu sublattice. It is known that the spinel $CuCr_2O_4$ [27] has a tetrahedral crystal structure and quenched magnetic frustration at room temperature, in which the magnetic moment of the Cu sublattice is FM while the interaction with the Cr sublattice becomes ferrimagnetic (FI). On the other hand, the negative Weiss constant is indicative of the dominance of the antiferromagnetic correlations from the Cr sublattice. In order to analyze the geometrical frustration, we also plotted

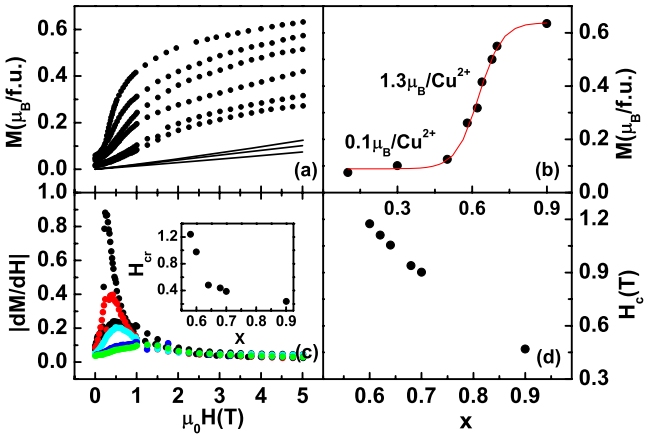

Figure 5. (a) The magnetic field dependence of magnetization for ZCCO compounds at 5 K. (b) The corresponding Cu content dependence of magnetic moment per formula at 5 T and 5 K. (c) The magnetic field dependence of $|\mathrm{d}M/\mathrm{d}H|$. The inset shows the corresponding Cu content dependence of metamagnetic transition field H_{cr} at 5 K. (d) The Cu content dependence of coercive field of H_c for ZCCO compounds at 5 K.

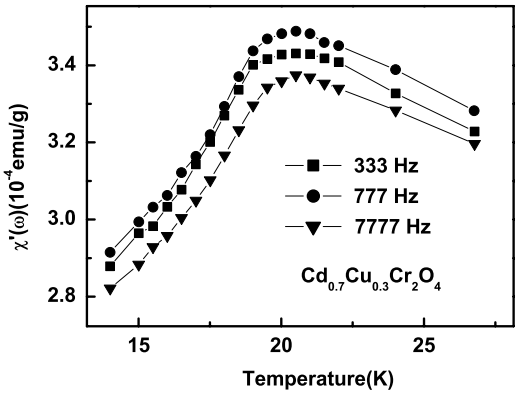

Figure 6. Temperature dependence of $\chi'(\omega, T)$ for $\omega/2\pi = 333$, 777 and 7777 Hz for $Zn_{0.7}Cu_{0.3}Cr_2O_4$.

the frustrated factor $f = |T_{CW}/T_N|$ versus x in figure 4. It is then found that the strong frustration of $ZnCr_2O_4$ turns out to be suppressed with Cu content, which has also been attained in CCCO system and could be ascribed to the 'pinning effect' of the Cu sublattice on the geometrical frustrated spins. Based on the formula $\mu_{eff} = (3\ k_B C/N_A)^{1/2}$ (k_B and N_A being the Boltzmann constant and the Avogadro number), the effective magnetic moment μ_{eff} can also be determined (see the inset of figure 4). The value of μ_{eff} decreases with Cu content while the theoretical value, according to the formula $2[s(s+1)]1/2\ \mu_B$ (3.87 μ_B and 1.73 μ_B for Cr^{3+} and Cu^{2+} ions with spin $s = 3/2$ and $1/2$, respectively), slightly increases. The experimental values of μ_{eff} are lower than the theoretical evaluation, which must originate from the short-range interaction in the paramagnetic region. Additionally, the trend discrepancy between the measured and theoretical values implies an enhanced magnetic correlation with Cu content above the Néel temperature and a formation of step grown FI clusters.

Figure 5(a) shows the isothermal magnetization measurements at 5 K for all samples. For the samples with $x \leqslant 0.5$, M varies nearly linearly and nonhysteretically with H, characteristic of dominance by antiferromagnets. For $x \geqslant 0.58$, a curvature appears beyond ~1 T together with an observable S-type behavior. The hysteretic behavior and the absent saturation tendency for the samples with $0.58 \leqslant x \leqslant 0.90$ imply a coexistence of AFM and FM coupling, thereby pointing towards SG or cluster glass freezing. The magnetization values at 5 T increase with x at a rate of 0.1 μ_B per Cu^{2+} ion for the samples with $0.1 \leqslant x \leqslant 0.5$, smaller than the expected saturation moment, 1 μ_B, implying the absence of a long-range-ordered ferromagnetic Cu sublattice. However, for the samples with $0.58 \leqslant x \leqslant 0.90$ (see figure 5(b)), 1.3 μ_B per Cu^{2+} ion is obtained, which is larger than the expected saturation moment, 1 μ_B, implying the existence of a parallel additive magnetic contribution to the Cu^{2+} ferromagnetic sublattice. A metamagnetic-like transition is observed at a critical field H_{cr} (defined as the maximum value of $|\mathrm{d}M/\mathrm{d}H|$) (see figure 5(c)). The value of H_{cr} is about 1.24 T at $x = 0.58$. Both H_{cr} (the inset of figure 5(c)) and the coercive field H_c (figure 5(d)) decrease with Cu content, which is in accordance with the released structural distortion with x in tetrahedral spinels. The magnetic anisotropy appears at $x = 0.58$ and it is reduced with further increasing Cu content, having the maximum value at $x = 0.58$.

The increasing A-site substitution results in the following effects by dc magnetic measurements. (i) The magnetic frustration is continuously suppressed with the Cu content, resulting from an increase of T_N and a decrease of $|\Theta_{CW}|$. (ii) The magnetization of the samples increases significantly with x. For tetrahedral-type spinels of ZCCO, an additive moment of 0.3 μ_B/f.u. is obtained with x, implying a pinning interaction of the Cu sublattice to the Cr frustrated magnetic lattice. (iii) The system is proposed to transform from AFM to SG-like state then to short-range-ordered cluster state with x. (iii) In tetrahedral-type ZCCO spinels of $0.58 \leqslant x \leqslant 0.90$, both the metamagnetic-like transition field H_{cr} and coercive field H_c are decreased with x, indicating the increasing Cu content reduces the magnetic anisotropy.

3.3. Ac susceptibility

In order to investigate the glassy magnetic property in ZCCO, ac susceptibility measurements, such as frequency and magnetic field dependence of transition temperature, are necessary. In this work, only the cubic spinels $Zn_{0.7}Cu_{0.3}Cr_2O_4$, $Zn_{0.5}Cu_{0.5}Cr_2O_4$ and tetragonal spinel $Zn_{0.1}Cu_{0.9}Cr_2O_4$ are discussed as examples. In figure 6 is presented the temperature dependence of the ZFC in-phase $\chi'(T)$ at different frequencies and an ac field of 5 Oe for $Zn_{0.7}Cu_{0.3}Cr_2O_4$. The peak amplitude decreases with (increasing) frequency. However, the peak temperature is frequency independent, indicating the predominance of AFM long-range ordering and the deficiency of the conventional SG-like state. Figure 7(a) presents the temperature dependence of the ZFC in-phase $\chi'(T)$ at different frequencies and with

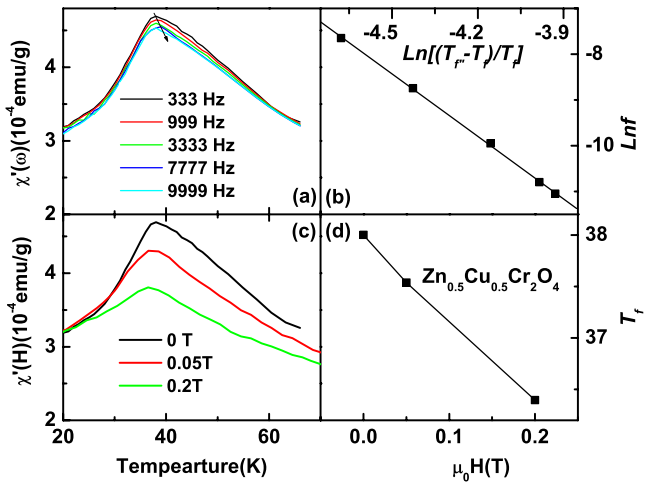

Figure 7. (a) Temperature dependence of $\chi'(\omega, T)$ for $\omega/2\pi = 333$, 999, 3333, 7777 and 9999 Hz for the $Zn_{0.5}Cu_{0.5}Cr_2O_4$ compound. (b) The corresponding measured freezing temperature $T_f(\omega, T)$ and the best fitted line by equation (1) for χ'. (c) Temperature dependence of $\chi'(H, T)$ measured at a frequency of 333 Hz under the magnetic fields of 0, 500 and 2000 Oe. (d) The corresponding experimental $T_f(H)$ values and the fitted data to equation (2).

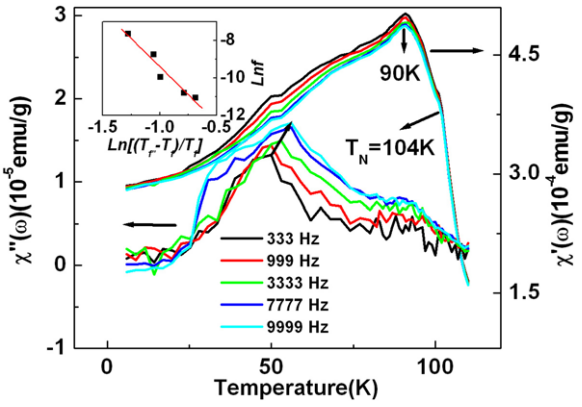

Figure 8. Temperature dependence of in-phase $\chi'(\omega, T)$ and out-of-phase $\chi''(\omega, T)$ ac susceptibilities measured at various frequencies of $\omega/2\pi = 333$, 999, 3333, 7777 and 9999 Hz for $Zn_{0.1}Cu_{0.9}Cr_2O_4$.The inset shows the measured freezing temperature $T_f(\omega, T)$ and the best fitted line by equation (1) for χ''.

an ac field of 5 Oe for $Zn_{0.5}Cu_{0.5}Cr_2O_4$. The $\chi'(T)$ curves display a peak at $T_f(\omega)$, which is frequency dependent, having the values 38, 38.10, 38.24, 38.35 and 38.39 K for $\omega/2\pi = 333$, 999, 3333, 7777 and 9999 Hz by Gaussian fitting to the peaks, respectively. The temperature of the peak, $T_f(\omega)$, shifts towards higher temperatures and the peak amplitude diminishes with increasing frequency. The value of the frequency sensitivity of $T_f(\omega)$, $\Delta T_f(\omega)/[T_f(\omega)\Delta \log_{10}\omega]$, has been used as a possible distinguishing criterion for the presence of a spin-glass phase [28, 31]. It is about 0.007 for $\chi'(\omega, T)$, lower than those reported for other typical insulating SG systems [31]. The divergence of the maximum relaxation time $\tau_{\max}$, occurring at the peak temperature, can be investigated by using conventional critical slowing down:

$$\frac{\tau}{\tau_0} = \xi^{-z\nu} = \left(\frac{T_f(\omega) - T_f}{T_f}\right)^{-z\nu}. \quad (1)$$

A best fit of the measured data to equation (1) is shown in figure 7(b), yielding the values $\tau_0 = 2.77 \times 10^{-13}$ s, $z\nu = 4.55$ and the transition temperature $T_f = 37.65$ K. Both values of τ_0 and $z\nu$ are the typical values for conventional spin glasses [32, 33]. However, $\tau_0 = 7.7 \times 10^{-10}$ s and $T_f = 36.86$ K are obtained by fitting to the Volgel–Fulcher scaling law (equation (2)),

$$\frac{\tau}{\tau_0} \propto \exp\frac{E_a}{k(T_f(\omega) - T_f)}. \quad (2)$$

The different dynamic scaling indicates, therefore, that there is a divergence of the SG relaxation time at a finite transition temperature, which demonstrates a phase transition from paramagnetism (PM) to SG-like combined with some small AFM clusters. Also, the existence of small AFM clusters can be confirmed by the shape of ac susceptibility peaks, which is not very sharp. Furthermore, it is well known that T_f shifts to lower temperature with the applied dc field in many classical SG systems, which can be well described by the Almeida–Thouless (AT) line [34].

$$T_f(H) = 1 - bH^{\delta}. \quad (3)$$

The temperature dependence of the ac susceptibility (in the in-phase component) under dc fields of 0, 500 and 2000 Oe measured at a frequency of 333 Hz is displayed in figure 7(c). Both the peak amplitude and the peak temperature decrease with increasing applied field. Figure 7(d) plots the experimental $T_f(H)$ values and the corresponding fitted data to equation (3). The fitted value of the exponent δ is 0.898, slightly larger than the value $\delta = 2/3$ given by the mean field theory prediction for SG [35, 36]. However, this is only a necessary (not a sufficient) feature of an SG transition [36]. For $Zn_{0.1}Cu_{0.9}Cr_2O_4$, as shown in figure 8, with decreasing temperature, the susceptibilities abruptly increase until the maximum at 90 K, showing at $T_N = 104$ K a small change in the upward trend; there is no frequency dependence for the peak of $\chi'(T)$ at 90 K, exhibiting the PM–FI phase transition. With decreasing temperature, the CG-like behavior is exposed by a shoulder in $\chi'(T)$ at $T_f' \approx 50$ K and a hump in $\chi''(T)$ at T_f'' as marked by the arrow in figure 8. T_f' and T_f'' are expected to be frequency dependent because of the CG-like freezing. The exact frequency dependence position of the shoulder in $\chi'(T)$, T_f', is rather difficult to determine. On the other hand, T_f'' shifts considerably to lower temperatures with decreasing frequency, with values $T_f'' \approx 47.7$, 50.3, 51.1, 54.3 and 56.1 K for $\omega/2\pi = 333$, 999, 3333, 7777 and 9999 Hz, respectively. The sensitivity of $T_f(\omega)$, $\Delta T_f(\omega)/[T_f(\omega)\Delta \log_{10}\omega]$, is about 0.119 for $\chi''(\omega, T)$, between the reported insulating SG, $(FeMg)Cl_2$, and superparamagnet, a-$(Ho_2O_3)(B_2O_3)$, indicating a CG-like freezing [31]. An attempt at fitting $T_f''(\omega/2\pi)$ data using equation (1) gives $\tau_0 = 2.11 \times 10^{-7}$ s and $z\nu = 5.979$ when $T_f = 37.3$ K is taken by fitting to the Volgel–Fulcher

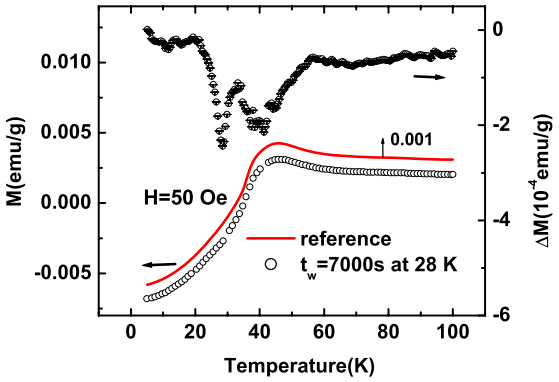

Figure 9. Temperature dependence of the reference magnetization $M_{\rm ref}$ (red solid line), the magnetization M (open circle), and $\Delta M = M - M_{\rm ref}$ (open circle with error bar) for the $Cd_{0.5}Cu_{0.5}Cr_2O_4$ compound. For clarity, the data for $M_{\rm ref}$ are shifted up by 0.001 emu g^{-1}.

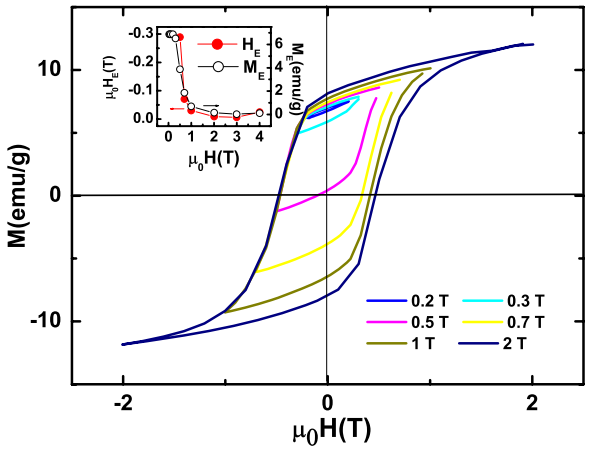

Figure 10. The FC (in 200 Oe) hysteresis loops for $Zn_{0.1}Cu_{0.9}Cr_2O_4$ at 5 K with different measuring magnetic fields. Inset: measuring field dependence of H_E and M_E at 5 K.

scaling law equation (2). The large relaxation time implies a freezing process of large size cluster glass at T_f''. The above ac susceptibility results show that the cubic spinel of ZCCO presents an SG-like behavior while the tetrahedral one exhibits a coexistence of FI and CG-like behavior.

3.4. Memory effect

To further probe the nature of the glassy behavior in ZCCO spinels, the time response of dc magnetization is important to reveal the spin dynamics [37]. In this work, we demonstrate the characteristic behaviors of glassiness by the memory effect for $Cd_{0.5}Cu_{0.5}Cr_2O_4$. It was studied by employing a dc magnetization method that was originally developed for the study of interacting glassy systems [38, 39]. In an SG or a system of interacting magnetic particles (but not in noninteracting particles), a dip appears on reheating at the temperature at which the sample was stopped under zero field.

The sample was first zero field cooled (ZFC) from 300 to 5 K continuously at a cooling rate of 2 K min^{-1}. After reaching the bottom temperature, a 50 Oe field was applied and the magnetization was measured on heating at the same rate up to 100 K. This M–T curve was taken as the reference curve, shown as a solid line in figure 9. Then, the sample was cooled again from 300 to 5 K at the same rate in zero field but with a temporary stop at 28 K for a time $t_w = 7000$ s. Finally, the magnetization in a 50 Oe field was recorded again during heating. The obtained results are shown in figure 9. The difference between the two $M(T)$ curves with experimental errors of measurements, $M = M(T) - M_{\rm ref}(T)$, is also shown in figure 9. A minimum is observed at the stop temperature 28 K, reflecting the memory effect. Additionally, another dip also appears around the SG-like freezing temperature of 38 K. The reason is still unclear. An identical measurement procedure at 30 K was also performed for the sample with $x = 0.9$. However, we have not observed any dip in the difference between two $M(T)$ curves, implying an existence of noninteracting superferrimagnetic-like clusters. The behavior of the memory effect for $x = 0.5$ and $x = 0.9$ suggests an evolvement of glassy behavior from interacting particles to superferrimagnetic-like clusters with Cu content.

3.5. Exchange-bias-like effect

If the ground state in tetragonal spinel is a true CG with superferrimagnetic clusters, the EB-like effect should be observed [40, 41]. For simplicity, only experiments performed on a sample of $Zn_{0.1}Cu_{0.9}Cr_2O_4$ with the low magnetic anisotropy among the tetrahedral ZCCO cases was discussed, although similar effects were also observed in other tetrahedral ZCCO compositions. Figure 10 shows the influence of measuring field on the exchange bias for $Zn_{0.1}Cu_{0.9}Cr_2O_4$. For each measurement, the sample was cooled under a field of 200 Oe from 300 to 5 K, then the hysteresis loops were measured between ±0.02, ±0.05, ±0.1, ±0.2, ±0.3, ±0.5, ±0.7, ±1, ±2, ±3, ±4 and ±5 T. For clarity, only the loops between ±0.2, ±0.3, ±0.5, ±0.7, ±1, ±2 T are presented in figure 10. When the measuring field was small ($H \leqslant 1$ T), the FC hysteresis loops always shifted to the negative field and positive magnetization, suggesting that a unidirectional anisotropy existed after the field cooling. However, when the measuring field was high enough, $H \geqslant 2$ T, the FC hysteresis loops did not show any shift, i.e. the EB-like effect disappears at high magnetic fields. The inset of figure 10 shows the measuring field dependence of the exchange bias field, $H_{\rm E}$, and the magnetization shift, $M_{\rm E}$. $H_{\rm E}$ is defined as the middle point between the negative field and the positive field at which the magnetization is equal to zero, and $M_{\rm E}$ is defined as the middle value between the two intersection points of the magnetization with $\mu_0 H = 0$ T. These shifts decrease rapidly with increasing applied magnetic field and disappear around 2 T. It is known that the EB in the AFM/FM systems only shifts in the direction of the field axis [42]. Thus, this EB-like effect in $Cu_{0.9}Zn_{0.1}Cr_2O_4$ must be derived from the freezing effect of the random anisotropy in the CG, rather than the coupling effect at the interfaces of the FM/AFM. The spins of the cluster are aligned to the field upon field cooling. The above EB-like measurements provide some evidence of the freezing of superferrimagnetic-like clusters with random anisotropy at lower temperatures, forming a CG-like ground state. Random anisotropy of FI clusters causes an EB-like effect in the tetrahedral spinel samples.

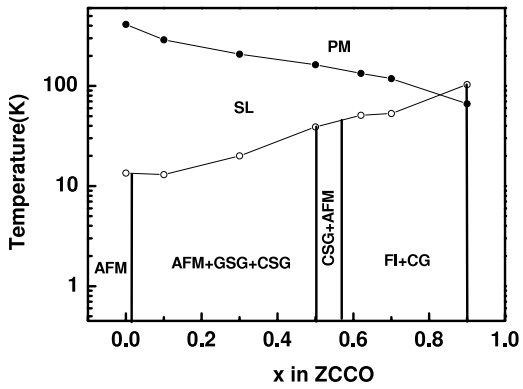

Figure 11. Doping temperature (x–T) schematic phase diagram of $Zn_{1-x}Cu_xCr_2O_4$, where x is the nominal Cu concentration.

4. Discussion

The above results confirm that cubic spinels ZCCO ($x \leqslant 0.50$) show an SG-like behavior while tetrahedral spinels ZCCO ($0.58 \leqslant x \leqslant 0.90$) exhibit a coexistence of FI and CG-like behavior. In order to understand the physics associated with A-site magnetic ion substitution in geometrical frustrated spinels ACr_2O_4, we have constructed a schematic phase diagram of ZCCO (see figure 11). A geometrically frustrated antiferromagnet presents a paramagnetic spin liquid (SL) state between T_N and $|T_{CW}|$ [43, 44]. It would be expected that, for lower Cu concentration below 50%, AFM order is dominant, coexisting with geometrical SG (GSG) and conventional SG (CSG) at low temperatures. The GSG component decreases with increasing Cu content and disappears at $x = 0.5$ based on the suppressed frustration factor. Thereafter, the FI cluster with glassy characteristics is dominant for copper concentration above 58% on the A site, exhibiting CG-like behavior below the freezing temperature. Our experiments only prove the existence of SG-like behavior for $x \leqslant 0.50$ and superferrimagnetic-like behavior for the sample with $x = 0.90$, and do not provide further CG-like evidence for other tetrahedral spinels or any definitive geometrical SG evidence. A detailed experiment measurement and analysis must be performed at the critical region.

In an ideal ZCCO compound, each Zn/Cu atom is surrounded by four oxygen atoms which build up a tetrahedron. Each Cr atom is surrounded by six oxygen atoms which build up an octahedron. A number of Zn atoms substituted by Cu introduces a magnetic moment that increases not only the crystal distortion but also the magnetic interactions. Here, a phase separation landscape due to the chemical inhomogeneous substitution on the A site is proposed for the ZCCO series by a schematic site percolation model [45–52]. Assuming that a low concentration of Cu^{2+} ions occupies the A sites in the $ZnCr_2O_4$ crystal lattices, there is an A-site disorder with the appearance of small Cu^{2+}-rich clusters and a chemical phase separation emerges. A small quantity of Cu^{2+}-rich clusters exhibits no interaction between them, ascribed to their long separation. Thus, the FM order percentage of the Cu sublattice is still low and the long-range AFM order predominates. But local Cu^{2+} ions with short-range-ordered FM have a pinning effect to the surrounding Cr sublattice, which induces a local released geometrical frustration, exhibiting a long-range-ordered AFM accompanied by a geometrical SG, as shown in $x = 0.3$. When the FM interaction is comparable to the AFM interaction, large site disorder and frustration appear, and finally no long-range ordering exists around the intermediate Cu concentration region, resulting in a conventional SG-like behavior with a few small AFM clusters, as shown in $x = 0.5$. At the nominal copper concentration $x = 0.58$, the increase of the A-site substitution makes the random oxygen displacements, originated from the ionic radius difference between Zn^{2+} and Cu^{2+} on the A site, become significant. It would enhance the random local radial distortions of the CrO_6 octahedron and reduce the Cu–Cu, Cu–Cr and Cu–O bond lengths. To reach the lowest energy state of the system, the structural phase transition occurs from the cubic to the tetrahedral lattice, where both Cu/ZnO_4 and CrO_6 polyhedra are distorted due to anisotropic atomic displacement of the oxygen atoms. In the tetrahedral structure, the Cu–Cu interaction is ferromagnetic, which brings about a pinning interaction to the complicated Cr magnetic sublattice. At the same time, the size of the FI cluster is expected to grow. The random anisotropy clusters with large grown size and the weak interaction between the clusters appear, exhibiting a collected FI order derived from the intracluster correlation and a CG-like behavior derived from the intercluster correlation.

Note that the magnetic property in $Zn_{0.5}Cu_{0.5}Cr_2O_4$ is different from $Cd_{0.5}Cu_{0.5}Cr_2O_4$. The former shows a conventional SG-like state and lacks any observation of magnetic phase separation induced by applied magnetic field. Considering similarities in the structure between them, it is obviously due to the different ionic radii between Zn^{2+} and Cd^{2+} ions. In $Cd_{0.5}Cu_{0.5}Cr_2O_4$, the larger ionic radii difference on the A site increases the distortion of the tetrahedron AO_4, resulting in a larger displacement of oxygen coordinates and off-center Cr^{3+}, which finally allows the AFM/FM magnetic phase separation induced by the more available pinning interaction [24]. A lower difference between A-site ionic radii, such as the ZCCO series, can be expected to be structurally and chemically more homogeneous, reflected in the structural phase transitions at the different critical concentrations of $x_{cu} = 0.58$ in ZCCO and $x_{cu} = 0.64$ in CCCO, which would reduce the probability of magnetic phase separation under external conditions. This suggests that the influence of the A-site disorder on the local structure distortion and magnetic behavior can be significant in a frustrated spinel magnet.

5. Conclusions

In conclusion, a series of chromium spinels, $Zn_{1-x}Cu_xCr_2O_4$, with an increasing A-site magnetic ionic substitution from 0.1 to 0.9, focused on $x = 0.5$ and 0.9, has been investigated using various experimental techniques. Our results have demonstrated that the samples with $x \leqslant 0.50$ have SG-like magnetic behavior with the cubic crystallographic structure and the samples with $x \geqslant 0.58$ have a coexistence of FI and CG-like magnetic behavior with the tetrahedral-type spinel

structure. A chemical phase separation scenario is taken to understand these experimental phenomena by a schematic site percolation model.

Acknowledgment

This work was supported by the National Natural Science Foundation of China (grant No 10505029).

References

[1] Ramirez A P 1994 *Annu. Rev. Mater. Sci.* **24** 453
[2] Martinez B, Labarta A, Rodriguez-Sola R and Obradors X 1994 *Phys. Rev.* B **50** 15779
[3] Harris M J, Bramwell S T, McMorrow D F, Zeiske T and Godfrey K W 1997 *Phys. Rev. Lett.* **79** 2554
[4] Zhang Z, Louca D, Visinoiu A, Lee S-H, Thompson J D, Proffen T, Llobet A, Qiu Y, Park S and Ueda Y 2006 *Phys. Rev.* B **74** 014108
[5] Lee S-H, Broholm C, Ratcliff W, Gasparovic G, Huang Q, Kim T H and Cheong S-W 2002 *Nature* **418** 856
[6] Lee S-H, Broholm C, Kim T H, Ratcliff W and Cheong S-W 2000 *Phys. Rev. Lett.* **84** 3718
[7] Sushkov A B, Tchernyshyov O, Ratcliff W, Cheong S and Drew H D 2005 *Phys. Rev. Lett.* **94** 137202
[8] Jo Y H, Park J-G, Kim H C, Ratcliff W and Cheong S-W 2005 *Phys. Rev.* B **72** 184421
[9] Yamashita Y and Ueda K 2000 *Phys. Rev. Lett.* **85** 4960
[10] Tchernyshyov O, Moessner R and Sondhi S L 2002 *Phys. Rev. Lett.* **88** 067203
[11] Lee S *et al* 2007 *J. Phys.: Condens. Matter* **19** 145259
[12] Nakamura H, Yoshimoto K, Shiga M, Nishi M and Kakurai K 1997 *J. Phys.: Condens. Matter* **9** 4701
[13] Lee S, Broholm C, Aeppli G, Ramirez A P, Perring T G, Carlile C J, Adams M, Jones T J L and Hessen B 1996 *Europhys. Lett.* **35** 127
[14] Belik A A, Tsujii N, Huang Q, Takayama-Muromachi E and Takano M 2007 *J. Phys.: Condens. Matter* **19** 145221
[15] Apetrei A, Mirebeau I, Goncharenko I, Andreica D and Bonville P 2006 *Phys. Rev. Lett.* **97** 206401
[16] Jana Y, Sakai O, Higashinaka R, Fukazawa H, Maeno1 Y, Dasgupta P and Ghosh D 2003 *Phys. Rev.* B **68** 174413
[17] Martinho H *et al* 2001 *Phys. Rev.* B **64** 024408
[18] Booth C, Gardner J, Kwei G, Heffner R H, Bridges F and Subramanian M A 2000 *Phys. Rev.* B **62** R755
[19] Tsui Y K, Burns C A, Snyder J and Schiffer P 1999 *Phys. Rev. Lett.* **82** 3532
[20] Seze L D 1977 *J. Phys. C: Solid State Phys.* **10** L353
[21] Villain J 1979 *Z. Phys.* B **33** 31
[22] Fiorani D, Viticoli S, Dormann J, Tholence J, Hammann J, Murani A and Soubeyroux J 1983 *J. Phys. C: Solid State Phys.* **16** 3175
[23] Yan L Q, Jiang Z W, Peng X D, He L H and Wang F W 2007 *Powder Diffract.* **22** 340
[24] Yan L Q, Yin W, Maciá F, He L and Wang F 2008 *Preprint* 0801.4298v1 [cond-mat]
[25] Chen W R, Zhang F C, Miao J, Xu B, Dong X L, Cao L X, Qiu X G and Zhao B R 2005 *Appl. Phys. Lett.* **87** 042508
[26] Rodrguez-Carvajal J 2003 *FullProf: A Program for Rietveld Refinement and Pattern Matching Analysis, Version 2.45 (Computer Software)* Laboratories Lon Brillouin (CEA-CNRS), Saclay, France
[27] Dollase W A and ONeill H St C 1997 *Acta Crystallogr.* C **53** 657
[28] Wu J and Leighton C 2003 *Phys. Rev.* B **67** 174408
[29] Nam D N H, Mathieu R, Nordblad P, Khiem N V and Phuc N X 2000 *Phys. Rev.* B **62** 8989
[30] Mandal P, Choudhury P, Biswas S K and Ghosh B 2004 *Phys. Rev.* B **70** 104407
[31] Mydosh J A 1993 *Spin Glass: An Experimental Introduction* (London: Taylor and Francis)
[32] Gunnarsson K, Svedlindh P, Nordblad P, Lundgren L, Aruga H and Ito A 1988 *Phys. Rev. Lett.* **61** 754
[33] Jonason K, Mattsson J and Nordblad P 1996 *Phys. Rev.* B **53** 6507
[34] de Almeida J R L and Thouless D J 1978 *J. Phys. A: Math. Gen.* **11** 983
[35] Fisher D and Sompolinsky H 1985 *Phys. Rev. Lett.* **54** 1063
[36] Nam D N H, Jonason K, Nordblad P, Khiem N V and Phuc N X 1999 *Phys. Rev.* B **59** 4189
[37] Binder K and Young A P 1986 *Rev. Mod. Phys.* **58** 801
[38] Bean C P and Livingston J D 1959 *J. Appl. Phys.* **30** 120
[39] Allia P, Coisson M, Knobel M, Tiberto P and Vinai F 1999 *Phys. Rev.* B **60** 12207
[40] Fiorani D, Bianco L D, Testa A and Trohidou K N 2006 *Phys. Rev.* B **73** 092403
[41] Fiorani D, Bianco L D and Testa A 2006 *J. Magn. Magn. Mater.* **300** 179
[42] Mukherjee S, Ranganathan R, Anilkumar P S and Joy P A 1996 *Phys. Rev.* B **54** 9267
[43] Rovers M T, Kyriakou P P, Dabkowska H A, Luke G M, Larkin M I and Savici A T 2002 *Phys. Rev.* B **66** 174434
[44] Ueda H, Katori H A, Mitamura H, Goto T and Takagi H 2005 *Phys. Rev. Lett.* **94** 047202
[45] Ballesteros H G, Fernandez L, Martin-Mayor V, Sudupe A, Parisi G and Ruiz-Lorenzo J 1999 *J. Phys. A: Math. Gen.* **32** 1
[46] Scarpetta S, de Candia A and Coniglio A 1997 *Phys. Rev.* E **55** 4943
[47] Misra S K and Orhun U 1992 *J. Phys: Condens. Matter* **4** 6459
[48] Fazileh F, Gooding R J and Johnston D C 2004 *Phys. Rev.* B **69** 104503
[49] Grinchuk P 2007 *Phys. Rev.* E **75** 041118
[50] Stauffer D and Aharony A 1992 *Introduction to Percolation Theory* (London: Taylor and Francis)
[51] Sahimi M 1994 *Applications of Percolation Theory* (London: Taylor and Francis)
[52] Deng Y and te H W J B 2005 *Phys. Rev.* E **72** 016126